



HAL
open science

Release of Evaluated $^{239}\text{Pu}(n,f)$ Prompt Fission Neutron Spectra Including the CEA and Chi-Nu High-precision Experimental Data

Denise Neudecker,, Keegan J. Kelly, Paola Marini

► **To cite this version:**

Denise Neudecker,, Keegan J. Kelly, Paola Marini. Release of Evaluated $^{239}\text{Pu}(n,f)$ Prompt Fission Neutron Spectra Including the CEA and Chi-Nu High-precision Experimental Data. 2022. hal-03823245

HAL Id: hal-03823245

<https://hal.science/hal-03823245v1>

Preprint submitted on 20 Oct 2022

HAL is a multi-disciplinary open access archive for the deposit and dissemination of scientific research documents, whether they are published or not. The documents may come from teaching and research institutions in France or abroad, or from public or private research centers.

L'archive ouverte pluridisciplinaire **HAL**, est destinée au dépôt et à la diffusion de documents scientifiques de niveau recherche, publiés ou non, émanant des établissements d'enseignement et de recherche français ou étrangers, des laboratoires publics ou privés.

LA-UR-22-23754

Approved for public release; distribution is unlimited.

Title: Release of Evaluated $^{239}\text{Pu}(n,f)$ Prompt Fission Neutron Spectra Including the CEA and Chi-Nu High-precision Experimental Data

Author(s): Neudecker, Denise
Kelly, Keegan John
Marini, Paola

Intended for: Report
Web

Issued: 2022-04-22



Los Alamos National Laboratory, an affirmative action/equal opportunity employer, is operated by Triad National Security, LLC for the National Nuclear Security Administration of U.S. Department of Energy under contract 89233218CNA000001. By approving this article, the publisher recognizes that the U.S. Government retains nonexclusive, royalty-free license to publish or reproduce the published form of this contribution, or to allow others to do so, for U.S. Government purposes. Los Alamos National Laboratory requests that the publisher identify this article as work performed under the auspices of the U.S. Department of Energy. Los Alamos National Laboratory strongly supports academic freedom and a researcher's right to publish; as an institution, however, the Laboratory does not endorse the viewpoint of a publication or guarantee its technical correctness.

Release of Evaluated $^{239}\text{Pu}(\text{n},\text{f})$ Prompt Fission Neutron Spectra Including the CEA and Chi-Nu High-precision Experimental Data

D. Neudecker^a, K.J. Kelly^a, P. Marini^b

^aLos Alamos National Laboratory, Los Alamos, NM, 87545, USA,

^bUniv. Bordeaux, CNRS, CENBG, UMR 5797, F-33170 Gradignan, France

April 19, 2022

Contents

1	Introduction	2
2	Evaluation Input: Similarities and Differences Compared to ENDF/B-VIII.0	2
3	Evaluated Results	4
3.1	Evaluated Results for $^{239}\text{Pu}(\text{n},\text{f})$ PFNS	4
3.2	Evaluated Mean Energies of $^{239}\text{Pu}(\text{n},\text{f})$ PFNS	4
3.3	Ratios of $^{239}\text{Pu}(\text{n},\text{f})/^{235}\text{U}(\text{n},\text{f})$ PFNS	9
4	Validation Results	9
4.1	Neutron Multiplication Factor of Selected Fast ICSBEP Critical Assemblies	10
4.2	Spectral Indexes in Jezebel and Flattop Critical Assemblies	12
4.3	LLNL Pulsed-sphere Neutron-leakage Spectra	12
5	Conclusions and Outlook	12

Abstract

This report documents an evaluation of ^{239}Pu prompt fission neutron spectra (PFNS) that is a release candidate for the upcoming U.S. nuclear data library, ENDF/B-VIII.1. This evaluation differs from its predecessor, ENDF/B-VIII.0, mainly by the inclusion of two ^{239}Pu PFNS high-precision experiments: one measured by the Chi-Nu team of LANL and LLNL, and the second one by the CEA team using the liquid-scintillator Chi-Nu array. These two data sets are the first ones that cover the ^{239}Pu PFNS for continuous incident-neutron energies of 1–20 MeV and broad outgoing-neutron energies with high precision. Chi-Nu covers outgoing-neutron energies from 10 keV–10 MeV, while CEA data are given for 0.25–11.3175 MeV. Previous data sets were either measured in a limited energy range or with less precision. Hence, these new CEA and Chi-Nu data provide decisive information for the evaluation. The resulting evaluated data correspond well to the new experimental PFNS, but are distinctly different than ENDF/B-VIII.0 values at all incident-neutron energies. These large differences compared to ENDF/B-VIII.0 can also be seen in the average mean energies computed from the new evaluated PFNS. However, the evaluated mean energies agree well with experimental data from Chi-Nu and CEA data, again, indicating that while the changes are large compared to ENDF/B-VIII.0, they are supported by experimental data. Due to those differences, large drops (e.g., -128 pcm for Jezebel or -114 for Flattop-Plutonium) in the predicted effective neutron multiplication factor, k_{eff} , of selected ICSBEP critical assemblies can be observed when these new PFNS are used compared to using ENDF/B-VIII.0. These large changes can be counter-balanced by considering, in addition to the new ^{239}Pu PFNS, new evaluated data for the neutron-induced ^{239}Pu fission cross section from the Neutron Data Standards project and the

average prompt fission neutron multiplicity from an NCSP project. A further indication that the evaluated data describe high-precision experimental data well is that the the evaluated PFNS also produce $^{239}\text{Pu}/^{235}\text{U}$ PFNS in agreement with associated Chi-Nu data. Changes in the simulation of ^{239}Pu LLNL pulsed-sphere neutron-leakage spectra are modest compared to ENDF/B-VIII.0 PFNS.

Keywords: ^{239}Pu , Prompt Fission Neutron Spectrum, ENDF/B-VIII.1.

LA-UR-22-

1 Introduction

This report serves as documentation for an evaluation of ^{239}Pu prompt fission neutron spectra (PFNS); this evaluation is a release candidate for the upcoming U.S. nuclear data library, ENDF/B-VIII.1. The PFNS described here are currently being tested as part of the IAEA-coordinated INDEN and LANL ^{239}Pu evaluation projects. It is also related to a FY2022 NCSP (Nuclear Criticality Safety Program) milestone: “ ^{235}U , ^{239}Pu : Evaluate PFNS and multiplicity consistently, including angular information about prompt neutrons”. The goal was to use the CGMF code [1] for consistently modeling the average prompt-neutron multiplicity, $\bar{\nu}_p$, and PFNS. Amy E. Lovell and the first author succeeded in obtaining evaluation-quality $\bar{\nu}_p$ for both isotopes [2, 3], but modeling the PFNS such that evaluation-quality nuclear data are obtained, remains elusive [4]. Therefore, an extended Los Alamos model was used [5] to model ^{235}U and ^{239}Pu PFNS and led to evaluation-quality nuclear data. The evaluation of ^{235}U PFNS is documented in Ref. [6], while this report focuses on ^{239}Pu PFNS.

The evaluation builds upon one undertaken for ENDF/B-VIII.0 [5] and initial studies in Ref. [7]. The main difference of this evaluation from ENDF/B-VIII.0 [8] was the inclusion of the final Chi-Nu and CEA experimental data [9–11] that were not yet available for ENDF/B-VIII.0. These new data set represent the culmination of many years of work from the LANL-LLNL Chi-Nu team and CEA/NNSA collaboration; both teams aimed at providing decisive experimental data for ^{239}Pu PFNS for a broad incident- and outgoing-neutron energy range, E_{inc} and E_{out} , respectively. Both teams succeeded in providing high-precision data for $E_{\text{inc}}=1\text{--}20$ MeV. Chi-Nu covers outgoing-neutron energies from 10 keV–10 MeV, while CEA data are given for 0.25–11.3175 MeV. In addition to that, the quality of the data allowed to observe for the first time many physics-expected features such as structures in PFNS around multiple-chance fission thresholds and commensurate with the pre-equilibrium neutron-emission process. Including these data into an evaluation, and sub-sequently into a nuclear-data library, makes that improved physics understanding of PFNS available to nuclear-data users.

The report here serves to document this new evaluation and its input. Section 2 summarizes the evaluation input and assumptions made in contrast to those for ENDF/B-VIII.0. Evaluated results for PFNS and mean energies are shown in Section 3. It is shown in Section 4 that evaluated PFNS including CEA and Chi-Nu data lead to large drops (more than 100 pcm) in fast ICSBEP critical assemblies [12] that need to be counter-balanced with improved evaluations of the average prompt fission neutron multiplicity, $\bar{\nu}_p$, [3] and improved fission cross-section evaluations [13, 14]. Predictions of LLNL pulsed-sphere neutron-leakage spectra [15] and spectral indexes calculated in the Jezebel and Flattop critical assemblies [12] differ only little from the values calculated with ENDF/B-VIII.0. Section 5 summarizes the main findings and provides an outlook.

2 Evaluation Input: Similarities and Differences Compared to ENDF/B-VIII.0

The evaluation for ENDF/B-VIII.0 for incident-neutron energies above 5 MeV was described in detail in Ref. [5, 7]. It forms the basis for this evaluation. We describe below what is the same and what is

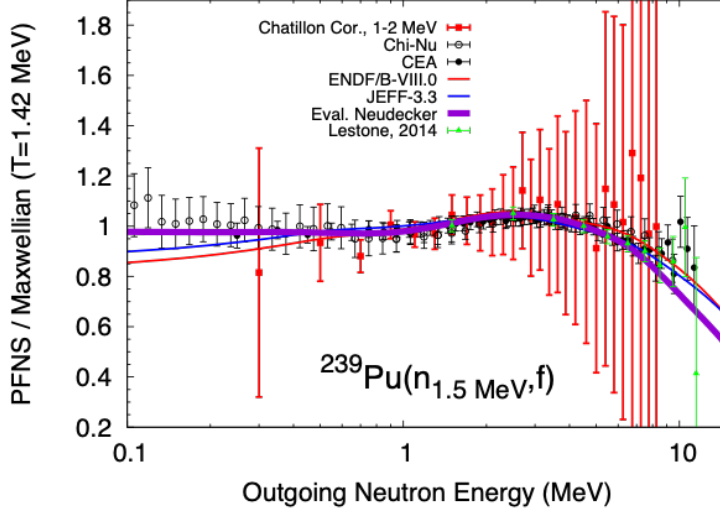


Figure 1: Evaluated PFNS for $E_{\text{inc}} = 1.5$ MeV are shown if the model prior from ENDF/B-VIII.0 is used with correlations across all E_{inc} . The new evaluated shape (purple line) above 8 MeV is lower than any experimental data.

different.

Evaluation algorithm and codes

The same evaluation methodology was employed for this evaluation and ENDF/B-VIII.0, namely, generalized least squares in PFNS space. The equation for the evaluation technique is given in Eqs. (11)–(14) of Ref. [5].

Even the same code was used for the evaluation of $E_{\text{inc}} > 2$ MeV. For $E_{\text{inc}} = 0.5$ –2 MeV, evaluated PFNS were obtained with the “EvaluateGLS” python module in ARIADNE [16]. The algorithm is the same in both codes. The only difference is that PFNS at several E_{inc} are evaluated concurrently for the evaluation at higher E_{inc} , while ARIADNE evaluates PFNS one E_{inc} at a time. This choice had been taken for the prior at $E_{\text{inc}} < 3$ MeV as strong model correlations across E_{inc} led to evaluated PFNS for $E_{\text{inc}} = 0.5$ –2 MeV being distinctly lower than CEA and Chi-Nu data at $E_{\text{out}} > 8$ MeV. This will be discussed in the paragraph on the prior input below.

Prior input

The same prior input as used for evaluating ENDF/B-VIII.0 ^{239}Pu PFNS for $E_{\text{inc}} > 5$ MeV (ENDF/B-VII.1 was retained for lower energies) was employed to obtain evaluated PFNS for $E_{\text{inc}} > 3$ MeV reported here as release candidate. For all other E_{inc} , evaluated PFNS differed from Chi-Nu and CEA experimental data for $E_{\text{out}} > 8$ MeV as shown in Fig. 1; the evaluated PFNS were lower than any of the experimental data.

The reason for these disagreements lies in a strongly-correlated prior and a slightly incorrect parameterization that is too far from Chi-Nu and experimental data at the second-chance fission threshold. No high-precision experimental PFNS were available to guide the prior estimate of Los Alamos model parameters, fission probabilities and the average total kinetic energy above 1.5 MeV. Fission barriers were fitted to ENDF/B-VII.0 fission probabilities, but there are large uncertainties on the parameter values. Hence, it is not surprising that the prior is too far from Chi-Nu data for $E_{\text{inc}} > 1.5$ MeV. The initial evaluation followed experimental data of CEA and Chi-Nu closely from 3–6 MeV, but, because of strong model correlations, led to the fact that high- E_{out} data for $E_{\text{inc}} < 3$ MeV were lower than experimental data.

To resolve this issue, model correlation across E_{inc} were set to zero for the evaluations at $E_{\text{inc}} < 3$ MeV; this is effectively the same as evaluating PFNS one E_{inc} at a time. The prior correlations as

well as uncertainties for the PFNS at one E_{inc} , however, remained the same. Due to these changes to the prior for $E_{\text{inc}} < 3$ MeV, evaluated PFNS were obtained (and are shown in Section 3.1) that are close to CEA and Chi-Nu experimental PFNS at all incident-neutron energies.

Experimental input The following experimental data were included in the evaluation:

- At ≈ 0.5 MeV: Knitter [17],
- At 1 MeV: CEA [10],
- At 1.5 MeV: Lestone [18, 19], CEA [10], Chatillon [20], Chi-Nu [9],
- At 2 MeV: Lestone [18, 19], CEA [10], Chatillon [20], Chi-Nu [9],
- > 2 MeV: CEA [10], Chatillon [20], Chi-Nu [9],

No thermal data are listed as no evaluation is provided at thermal; instead the INDEN evaluation based on only experimental data is recommended. It should be mentioned that Chatillon data were corrected following Ref. [21].

3 Evaluated Results

3.1 Evaluated Results for $^{239}\text{Pu}(\text{n},\text{f})$ PFNS

Evaluated PFNS from 0.5–5 MeV The evaluated results from 0.5–5 MeV (Figs. 2-3) correspond well to experimental data, but differ distinctly from ENDF/B-VIII.0 at nearly all E_{out} . The new evaluation follows experimental data better than ENDF/B-VIII.0; this can be easily understood as neither CEA nor Chi-Nu were available for ENDF/B-VIII.0. The new evaluation, however, lies mostly in the middle between CEA and Chi-Nu experimental data.

The effective neutron multiplication factor, k_{eff} , of ICSBEP critical assemblies is mostly sensitive to PFNS for $E_{\text{inc}} < 6$ MeV. Large differences in simulated k_{eff} are expected with the new PFNS given the distinct differences to those of ENDF/B-VIII.0.

Evaluated PFNS from 6–20 MeV Both, ENDF/B-VIII.0 and this evaluation, indicate the emergence of the second-chance fission structure at 6 MeV in Fig. 3. While ENDF/B-VIII.0 correctly predicted the E_{inc} at which second-chance fission opens up, it did not get the shape of the PFNS completely right given the lack of high-precision experimental data for ENDF/B-VIII.0. Hence, larger differences between ENDF/B-VIII.0 and this evaluation are observed at this E_{inc} .

Overall larger changes are observed from 5.5–20 MeV for ENDF/B-VIII.0 and the new evaluation due to CEA and Chi-Nu data in Figs. 3–5. Previously, only Chatillon data were available for $E_{\text{inc}} > 2$ MeV. These experimental data are too uncertain to clearly show structures arising due to pre-equilibrium neutron emission or multiple-chance fission. Hence, ENDF/B-VIII.0 relied on a model prior parameterization to describe these physics-expected structures. While the prior of ENDF/B-VIII.0 predicted the E_{out} and E_{inc} of the emergence of these structures correctly, it did not completely capture the shapes that we now see emerge from CEA and Chi-Nu experimental data. The final CEA and Chi-Nu data map these structures out with high precision, and lead to evaluated PFNS better reflecting the physics of this process.

3.2 Evaluated Mean Energies of $^{239}\text{Pu}(\text{n},\text{f})$ PFNS

The new evaluated mean energies in Fig. 6 follow Chi-Nu data within experimental uncertainties. CEA uncertainties are distinctly lower but the experimental data agree within uncertainties with Chi-Nu

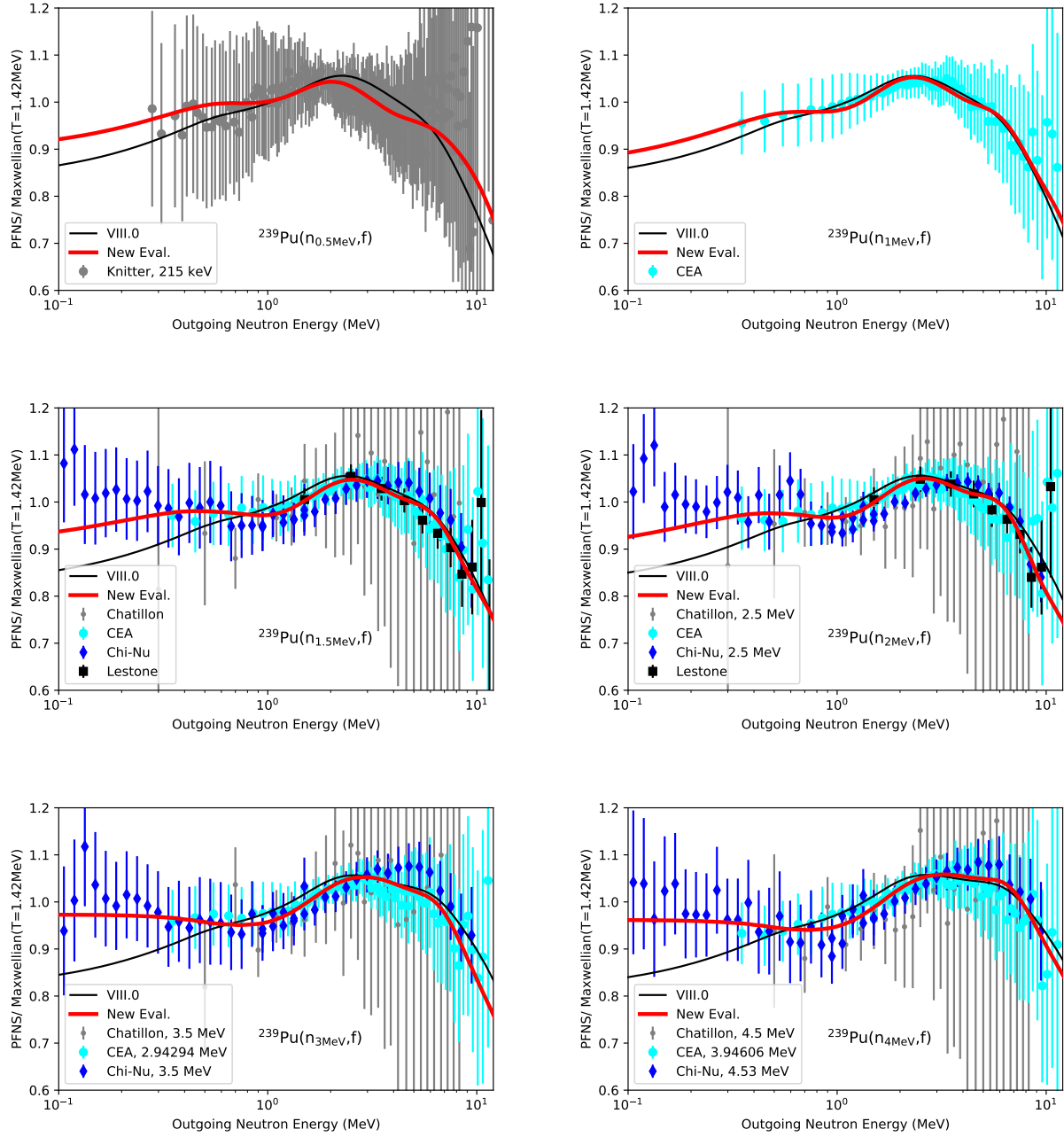


Figure 2: Final evaluated results are compared to ENDF/B-VIII.0 and available experimental data.

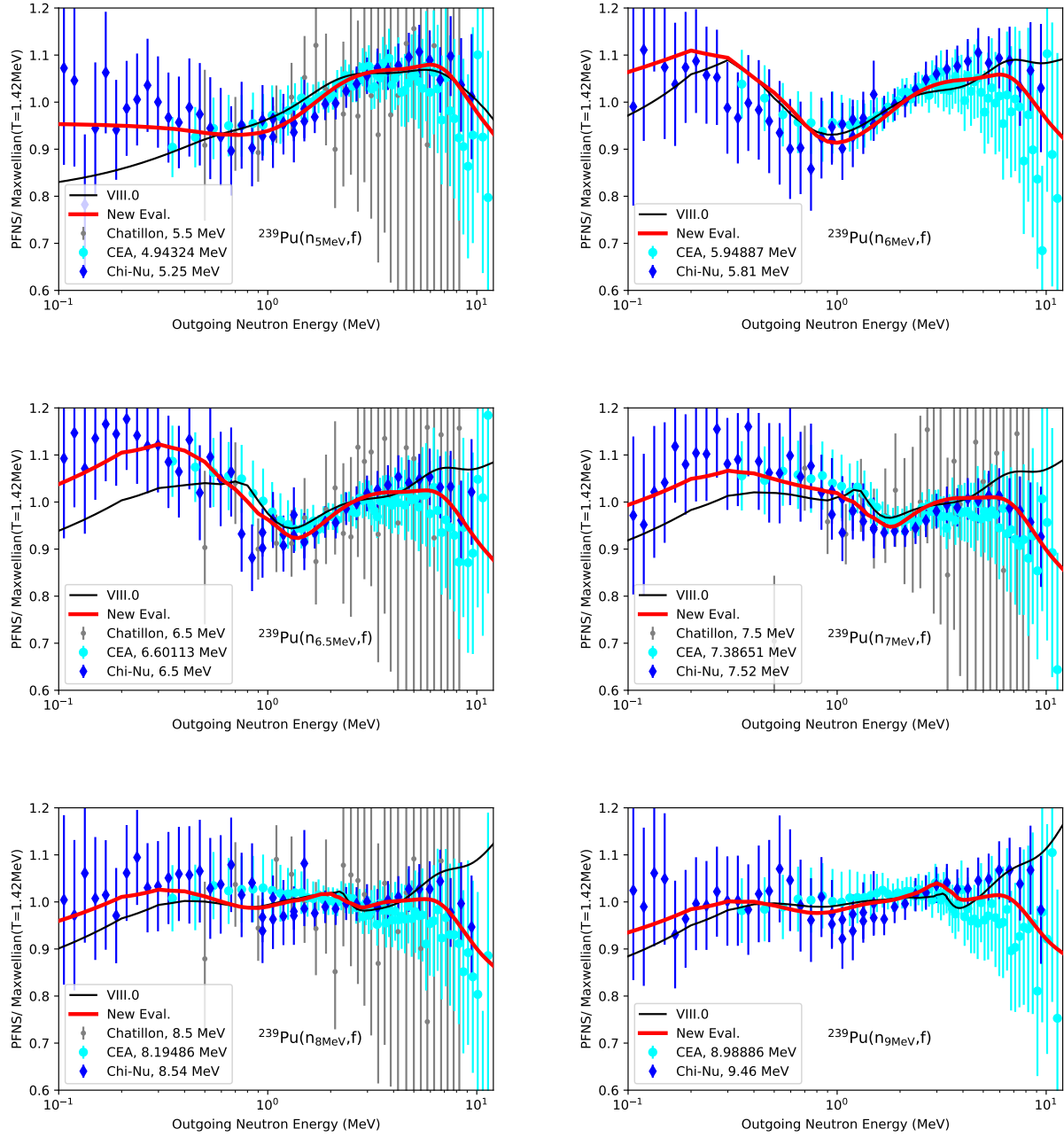


Figure 3: Final evaluated results are compared to ENDF/B-VIII.0 and available experimental data.

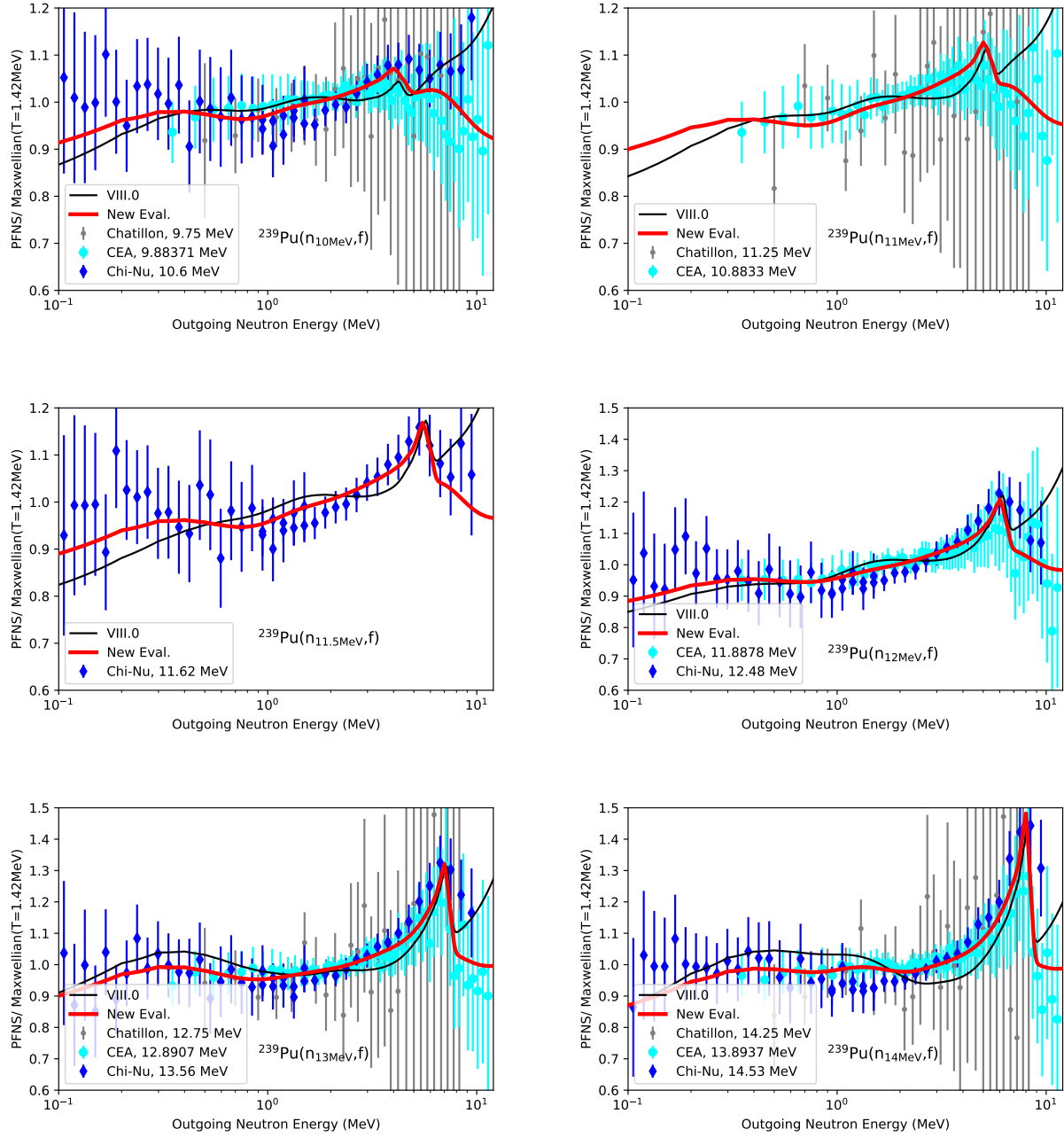


Figure 4: Final evaluated results are compared to ENDF/B-VIII.0 and available experimental data.

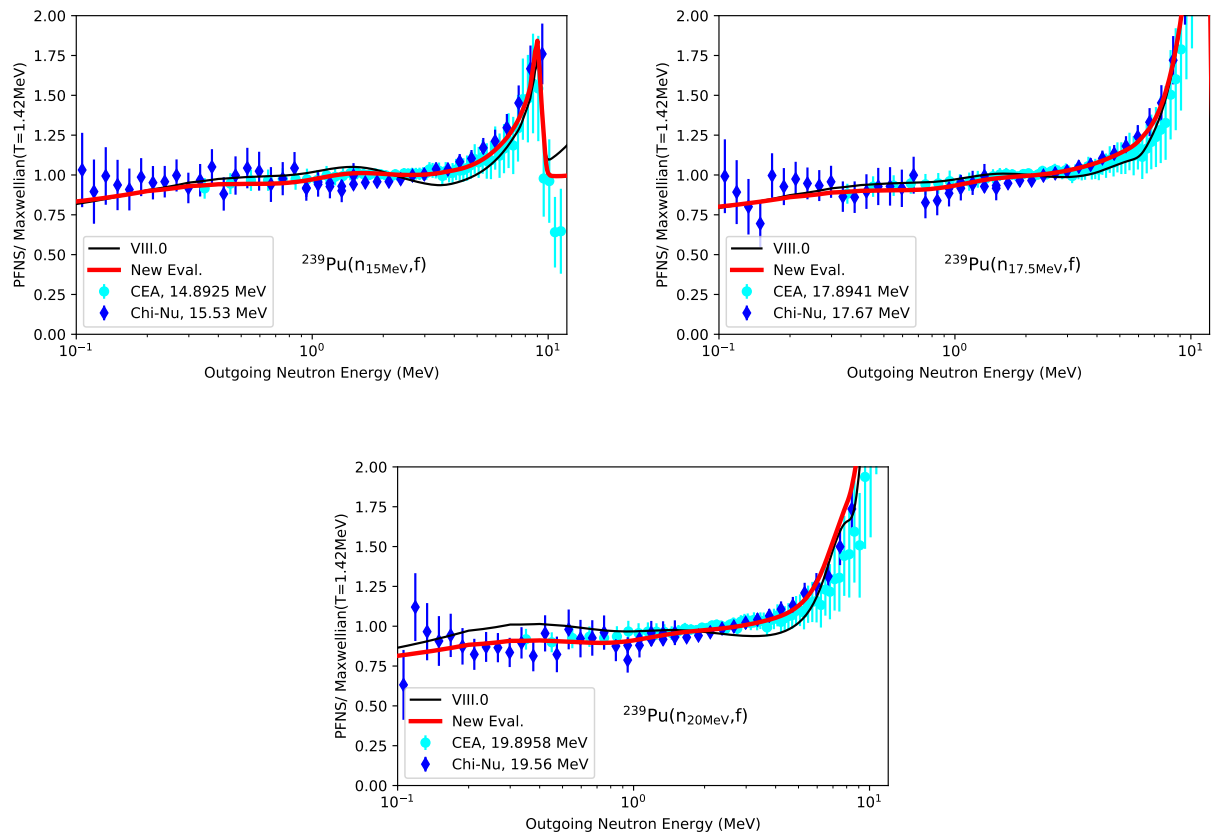


Figure 5: Final evaluated results are compared to ENDF/B-VIII.0 and available experimental data.

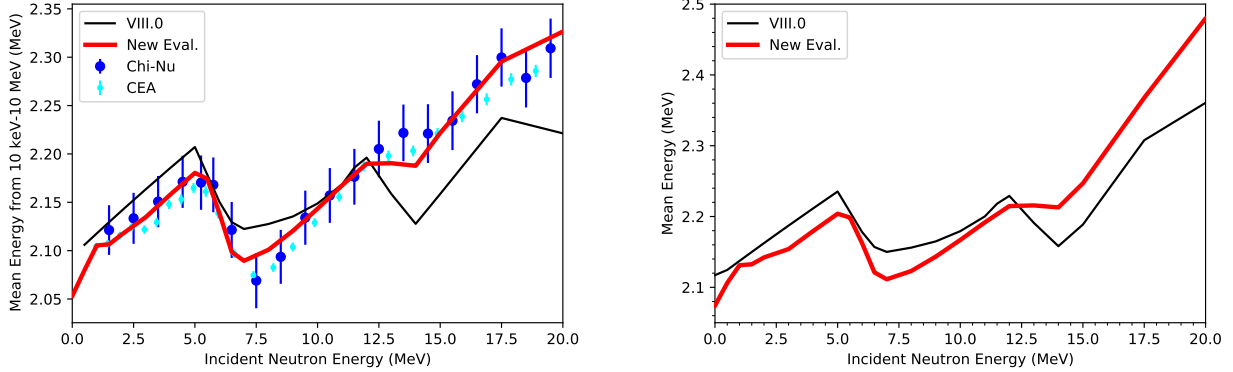


Figure 6: Final evaluated mean energies are compared to those of ENDF/B-VIII.0, CEA and Chi-Nu. It should be mentioned that CEA uncertainties shown are those reported by the experimentalists, while enlarged uncertainties were used for the evaluation.

data. It should be mentioned that CEA uncertainties shown are those reported by the experimentalists, while enlarged uncertainties, about the order of Chi-Nu uncertainties, were used for the evaluation. Hence, the evaluated mean energies are likely also within CEA uncertainties as used for the PFNS evaluation here.

The evaluated mean energies differ distinctly from ENDF/B-VIII.0 mean energies. at nearly all incident-neutron energies, with the exception of 5.5 MeV and 11 MeV. Again, large differences in k_{eff} can be expected from these different trends.

3.3 Ratios of $^{239}\text{Pu}(\text{n},\text{f})/^{235}\text{U}(\text{n},\text{f})$ PFNS

As mentioned before, new ^{235}U PFNS were evaluated with the LAM and Chi-Nu experimental data [6] and provided as a release candidate for ENDF/B-VIII.1. One can counter-check, together with this ^{239}Pu PFNS evaluation, whether the ratios of ^{239}Pu and ^{235}U compared still well to experimental data. The Chi-Nu team and Lestone et al. [18, 19] provided high-precision experimental data at $E_{\text{inc}}=1.5$ MeV for both, ^{239}Pu and ^{235}U PFNS. Sugimoto et al. [22] gave $^{239}\text{Pu}/^{235}\text{U}$ ratio PFNS at 0.4 MeV that were transposed in Fig. 7 to 1.5 MeV by P. Talou. These three ratio data sets yield a second reference point to counter-check whether evaluated results agree with experimental data.

Both, the ratios obtained from ENDF/B-VIII.0 and this evaluation, agree within the $1\text{-}\sigma$ uncertainties with these three data sets. The new evaluation is closer to experimental data below 1 MeV and from 1.5-5 MeV, while ENDF/B-VIII.0 describes experimental data better from 1-1.5 MeV. Above 5 MeV, there is considerable spread and/ or uncertainty in experimental data.

4 Validation Results

Validation results for three different evaluations are discussed:

1. ENDF/B-VIII.0,
2. ENDF/B-VIII.0 except for new PFNS for $E_{\text{inc}}=0.5\text{--}30$ MeV,
3. ENDF/B-VIII.0 except for new PFNS for $E_{\text{inc}}=0.5\text{--}30$ MeV, a new ^{239}Pu $\bar{\nu}_p$ from Refs. [3] and a new ^{239}Pu neutron-induced fission cross section from Refs. [13, 14].

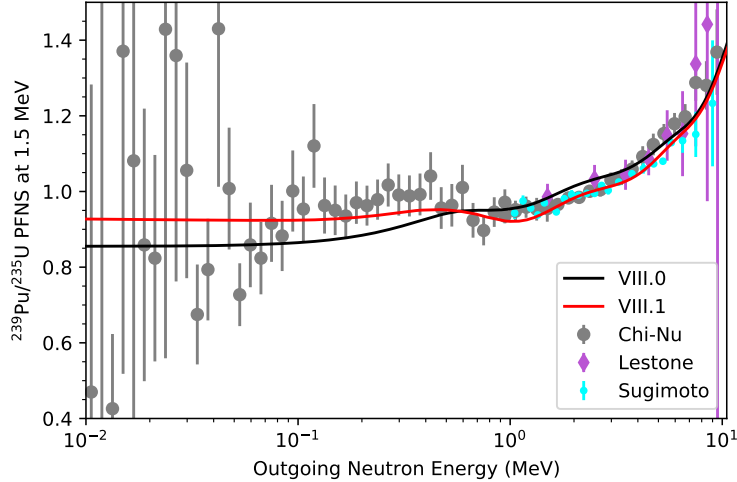


Figure 7: $^{239}\text{Pu}/^{235}\text{U}$ ratio PFNS for $E_{\text{inc}}=1.5$ MeV are shown for the new evaluation, ENDF/B-VIII.0 and experimental data.

An evaluation by the INDEN collaboration is used for the ^{239}Pu PFNS at thermal. The second evaluation combination was only used for simulations of k_{eff} of Jezebel and Flattop and associated reaction rates. All validation results were obtained by running MCNP-6.2 [23]. ENDF/B-VIII.0 was used for all other isotopes than ^{239}Pu .

4.1 Neutron Multiplication Factor of Selected Fast ICSBEP Critical Assemblies

It is shown in Table I that new PFNS lead to a considerable reduction of k_{eff} for the Jezebel and Flattop critical assemblies [12], by 128 and 114 pcm, respectively. These large changes agree with the fact that the new PFNS are distinctly softer than ENDF/B-VIII.0 for $E_{\text{inc}} < 5.5$ MeV. The critical assemblies studied are mostly sensitive to nuclear data below 5.5 MeV.

Such a large under-prediction of k_{eff} of Jezebel and Flattop critical assemblies is not acceptable for an ENDF/B libraries, and must be counter-balanced by changes in other observables. Around the same time this evaluation was finished, a new ^{239}Pu $\bar{\nu}_p$ from Refs. [3] and (n,f) cross-section evaluation became available [13,14]. Both evaluations include new high-precision data and experimental covariances enhanced by templates of expected measurement uncertainties, while $\bar{\nu}_p$ also includes detailed fission modeling from the CGMF code [1]. If these two new evaluations are considered together with the new ^{239}Pu PFNS, both Jezebel and Flattop k_{eff} are closer to ENDF/B-VIII.0 on a statistically significant level. This gave a first indication that the new physics gained through recent high-precision measurements and CGMF modeling as well as better uncertainty quantification led to a combination of nuclear data that reasonably predict k_{eff} .

This combination of nuclear data was further tested by simulating k_{eff} of selected ICSBEP critical assemblies as shown in Fig. 8. Overall, simulated k_{eff} values are close to those of ENDF/B-VIII.0. The C/E (calculated over experimental) values are better with this evaluation compared to ENDF/B-VIII.0 for assemblies with the hardest spectra, such as Jezebel (PMF001), dirty Jezebel (PMF002), or Flattop (PMF006), while they are worse for assemblies with softer spectra (e.g., PMF-044 series, or PMI003 and PMI004). The mean bias over ENDF/B-VIII.0 C/E values is 78 pcm, while it is 127 pcm for the evaluation combination presented here. Hence, small tweaks in $\bar{\nu}_p$ might be needed or the changes in k_{eff} might need to be counter-balanced with other observables, such as (n, γ), (n,el), or (n,inl) cross sections.

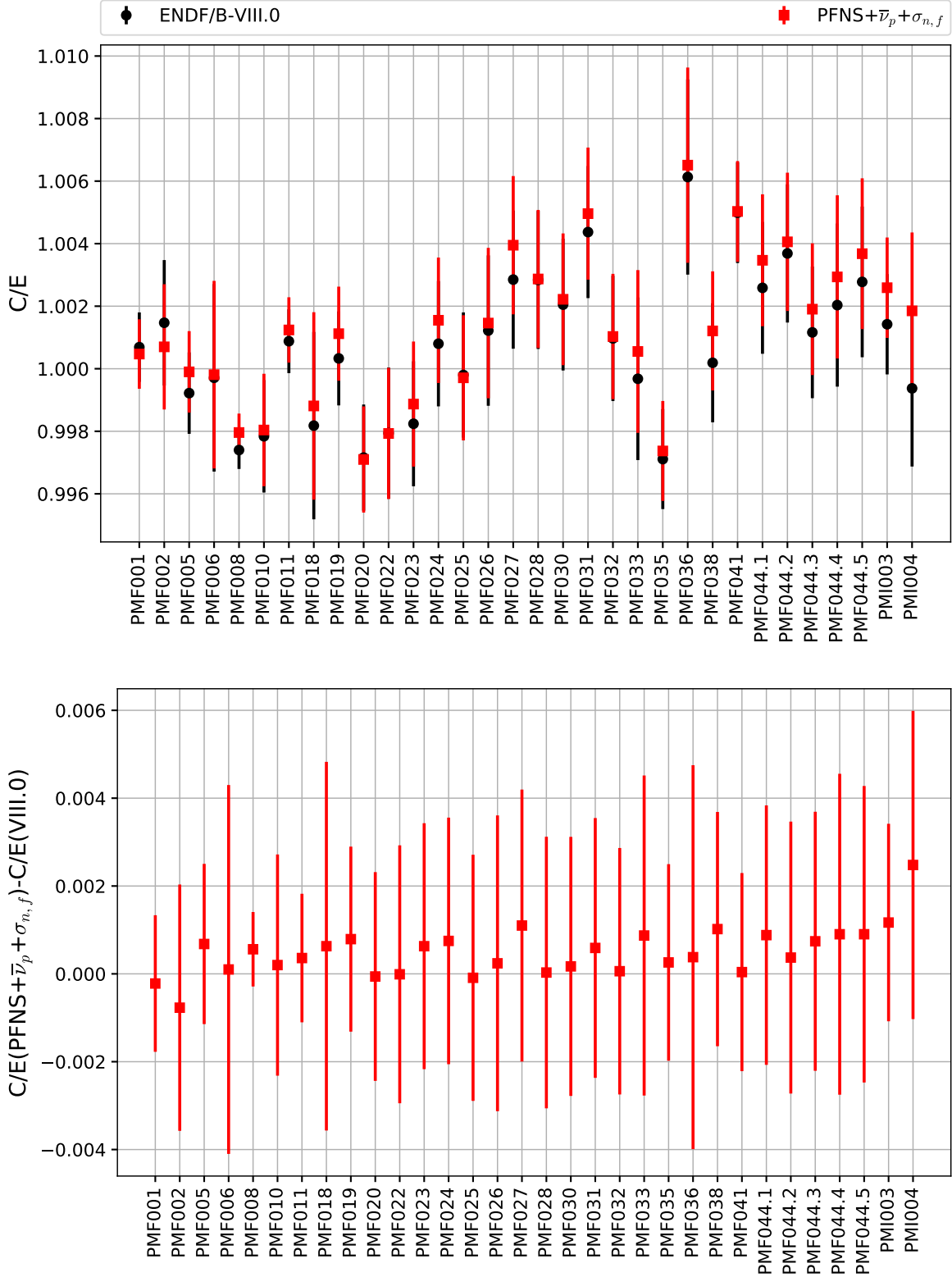


Figure 8: Simulated and experimental k_{eff} values for selected ICSBEP critical assemblies are compared with each other for ENDF/B-VIII.0 and ENDF/B-VIII.0 except for the new PFNS, $\bar{\nu}_p$ and (n,f) cross section. An abbreviated ICSBEP nomenclature is used.

Table I: Simulated values for k_{eff} and spectral indexes are compared with each other for ENDF/B-VIII.0, ENDF/B-VIII.0 with the new PFNS for $E_{\text{inc}}=0.5\text{--}30$ MeV and ENDF/B-VIII.0 with the new PFNS for $E_{\text{inc}}=0.5\text{--}30$ MeV, a NCSP $\bar{\nu}_p$ from Ref. [3] and a (n,f) cross section updated following Refs. [13, 14].

Benchmark	Observable	VIII.0	VIII.0+PFNS	VIII.0+PFNS+ $\bar{\nu}_p+\sigma_f$	
Jezebel	k_{eff}	1.00069(1)	0.99941(1)	1.00047(1)	
	$\frac{{}^{239}\text{Pu}\sigma_{n,2n}}{{}^{239}\text{Pu}\sigma_{n,f}}$	0.00230(5)	0.00225(5)	0.00224(5)	
	$\frac{{}^{239}\text{Pu}\sigma_{n,\gamma}}{{}^{239}\text{Pu}\sigma_{n,f}}$	0.0345(2)	0.0354(2)	0.0355(2)	
	$\frac{{}^{238}\text{U}\sigma_{n,f}}{{}^{235}\text{U}\sigma_{n,f}}$	0.212(1)	0.209(1)	0.209(1)	
	$\frac{{}^{237}\text{Np}\sigma_{n,f}}{{}^{235}\text{U}\sigma_{n,f}}$	0.9768(5)	0.9660(5)	0.9662(5)	
	$\frac{{}^{233}\text{U}\sigma_{n,f}}{{}^{235}\text{U}\sigma_{n,f}}$	1.566(7)	1.566(7)	1.566(7)	
	$\frac{{}^{239}\text{Pu}\sigma_{n,f}}{{}^{235}\text{U}\sigma_{n,f}}$	1.427(6)	1.424(6)	1.423(6)	
	Flattop-Pu	k_{eff}	0.99971(1)	0.99857(1)	0.99981(1)
		$\frac{{}^{239}\text{Pu}\sigma_{n,2n}}{{}^{239}\text{Pu}\sigma_{n,f}}$	0.00197(4)	0.00193(4)	0.00193(4)
		$\frac{{}^{239}\text{Pu}\sigma_{n,\gamma}}{{}^{239}\text{Pu}\sigma_{n,f}}$	0.0455(1)	0.0464(1)	0.0464(1)
$\frac{{}^{238}\text{U}\sigma_{n,f}}{{}^{235}\text{U}\sigma_{n,f}}$		0.1800(9)	0.1775(9)	0.1774(9)	
$\frac{{}^{237}\text{Np}\sigma_{n,f}}{{}^{235}\text{U}\sigma_{n,f}}$		0.8591(4)	0.8499(4)	0.8497(4)	

4.2 Spectral Indexes in Jezebel and Flattop Critical Assemblies

Spectral indexes in Jezebel and Flattop critical assemblies were calculated with all three combinations of files, ENDF/B-VIII.0, ENDF/B-VIII.0 including the new PFNS, and ENDF/B-VIII.0 and the new ${}^{239}\text{Pu}$ fission source term. The aim here was to test how close these values are to those predicted with ENDF/B-VIII.0. Simulated values using the new evaluations are close to ENDF/B-VIII.0 for ${}^{239}\text{Pu}(n,2n)/{}^{239}\text{Pu}(n,f)$, ${}^{238}\text{U}(n,f)/{}^{235}\text{U}(n,f)$, ${}^{233}\text{U}(n,f)/{}^{235}\text{U}(n,f)$, and ${}^{239}\text{Pu}(n,f)/{}^{235}\text{U}(n,f)$ in Jezebel and ${}^{239}\text{Pu}(n,2n)/{}^{239}\text{Pu}(n,f)$ in Flattop critical assemblies.

4.3 LLNL Pulsed-sphere Neutron-leakage Spectra

LLNL pulsed spheres [15] allow us to validate ${}^{239}\text{Pu}$ from approximately 10–15 MeV, where we also observed changes in $\bar{\nu}_p$, PFNS and (n,f) cross sections. These changes did not significantly impact the simulation of Pu LLNL pulsed spheres as can be seen in Fig. 9. This can be attributed to the modest changes in all three observables compared to the significant C/E bias in the simulated values, but also to the fact that changes in a narrow energy range in (n,f) cross section and $\bar{\nu}_p$ lead mostly to a constant off-set of the simulated neutron-leakage spectra [24]. As the experimental data are treated as shape data and are re-normalized to yield an integral of one over the entire spectrum, changes in $\bar{\nu}_p$ and (n,f) cross section have little effect.

5 Conclusions and Outlook

This report documents an evaluation of the ${}^{239}\text{Pu}$ PFNS that includes CEA and Chi-Nu experimental data [9–11]. Both measurement campaigns were undertaken at LANSCE using Chi-Nu neutron-detector arrays. The Chi-Nu campaign is a decade-long effort of LANL and LLNL to measure high-precision PFNS of actinides for the Office of Energy Sciences, while the CEA measurement was a CEA/NNSA effort. To make these data available to the transport community, final ${}^{239}\text{Pu}$ CEA and

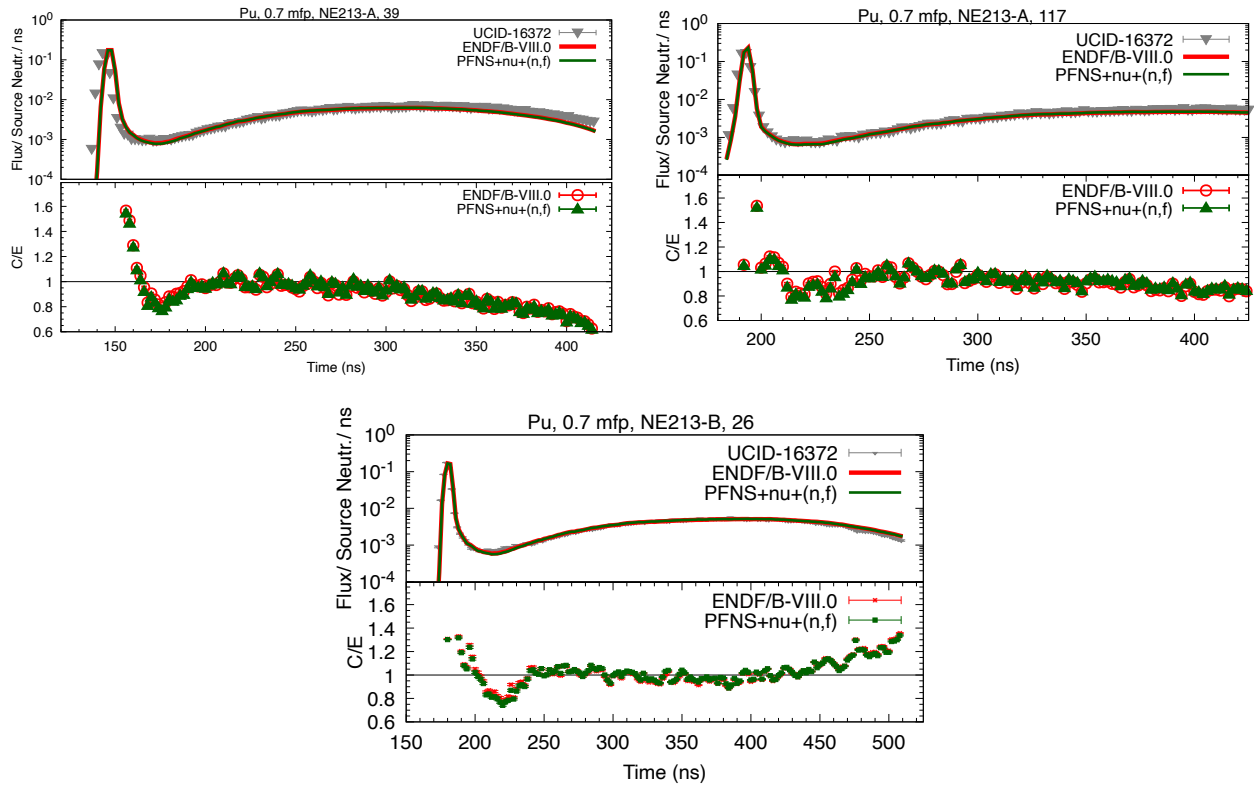


Figure 9: Calculated and experimental values are shown for Pu LLNL pulsed spheres. Calculated values are given for ENDF/B-VIII.0 as well as the new ^{239}Pu files including new $^{239}\text{Pu}(n,f)$ cross sections, PFNS and $\bar{\nu}_p$.

Chi-Nu experimental data were included into an evaluation using the Los Alamos model prior and experimental data used for the ENDF/B-VIII.0 evaluation [5]. These new evaluated PFNS correspond well to past experimental data as well as CEA and Chi-Nu data. The mean energies calculated from new PFNS agree within the experimental uncertainties with Chi-Nu mean energies and for the evaluation enlarged CEA uncertainties.

In addition to that, $^{239}\text{Pu}/^{235}\text{U}$ PFNS ratios at $E_{\text{inc}}=1.5$ MeV using two evaluations including final Chi-Nu data agree with three different data sets providing the same ratios, Chi-Nu, Lestone and Sugimoto data. The last data set was not included in any of the evaluations and, thus, showcases that both, the new ^{235}U and ^{239}Pu evaluations, are reasonable.

The new evaluated PFNS are distinctly softer than ENDF/B-VIII.0 for all E_{inc} . Due to that, these new PFNS significantly reduce the simulated effective neutron multiplication factor of selected fast and intermediate ICSBEP [12] critical assemblies compared to ENDF/B-VIII.0. This large drop in k_{eff} can be counter-balanced by considering new evaluations of the average prompt fission neutron multiplicity and the fission cross section which both encompass knowledge from recent high-precision measurement and better uncertainty quantification of experimental data [3, 13, 14].

The new evaluated PFNS also differ distinctly from ENDF/B-VIII.0 for $E_{\text{inc}} > 5.5$ MeV as CEA and Chi-Nu data provide for the first time decisive information on PFNS at these higher energies. However, the simulated ^{239}Pu LLNL pulsed-sphere neutron-leakage spectra [15] change only little.

These new evaluated PFNS were delivered to two ^{239}Pu evaluation collaborations, one by LANL and the other part of the IAEA-coordinated INDEN projects. Currently, these data are included in their ENDF/B-VIII.1 release files. If one of those evaluations is selected, these PFNS might become part of the ^{239}Pu ENDF/B-VIII.1 file. Thus, the new physics understanding gained through CEA and Chi-Nu PFNS could be delivered to the transport community through ENDF/B-VIII.1.

In the future, such evaluations might be undertaken primarily with modern PFNS models such as implemented in CGMF [1]. Work is ongoing to use this code for PFNS evaluations [4], but the model is not yet accurate enough to serve as a prior. Until then, the Los Alamos model will be used.

Point of contacts

DN serves as contact for the evaluation and validation, while KJK and PM serve as point of contacts on Chi-Nu and CEA experimental data and their analysis, respectively.

Acknowledgments

DN thanks Mark B. Chadwick (LANL) for insightful discussions on evaluated PFNS results. Work at LANL was carried out under the auspices of the National Nuclear Security Administration (NNSA) of the U.S. Department of Energy (DOE) under contract 89233218CNA000001. We gratefully acknowledge partial support of the Advanced Simulation and Computing program at LANL and the DOE Nuclear Criticality Safety Program, funded and managed by NNSA for the DOE.

References

- [1] P. Talou, T. Kawano, I. Stetcu et al. , “Fission Fragment Decay Simulations with the CGMF Code,” *COMP. PHYS. COMM.* **269**, 108087 (2021).
- [2] A.E. Lovell, D. Neudecker and P. Talou, “Release of Evaluated $^{235}\text{U}(n,f)$ Average Prompt Neutron Multiplicities Including the CGMF Model,” Los Alamos National Laboratory Report LA-UR-22-xxxx (2022).

- [3] D. Neudecker, A.E. Lovell and P. Talou, “Producing ENDF/B-quality Evaluations of $^{239}\text{Pu}(n,f)$ and $^{235}\text{U}(n,f)$ Average Prompt Neutron Multiplicities using the CGMF Model” Los Alamos National Laboratory Report LA-UR-21-29906 (2021).
- [4] A.E. Lovell and D. Neudecker, “Correcting the PFNS for more consistent fission modeling,” Los Alamos National Laboratory Report LA-UR-21- (2021).
- [5] D. Neudecker, P. Talou, T. Kawano et al. , “Evaluations of Energy Spectra of Neutrons Emitted Promptly in Neutron-induced Fission of ^{235}U and ^{239}Pu ,” NUCL. DATA SHEETS **148**, 293 (2018).
- [6] D. Neudecker and K.J. Kelly, “Including Chi-Nu ^{235}U PFNS Experimental Data into an ENDF/B-VIII. 1 Release Candidate Evaluation,” Los Alamos National Laboratory LA-UR-22-22220 (2022).” Los Alamos National Laboratory LA-UR-22-22220 (2022).
- [7] D. Neudecker, P. Talou, T. Kawano et al. , “Evaluation of the ^{239}Pu prompt fission neutron spectrum induced by neutrons of 500 keV and associated covariances,” NUCLEAR INSTRUMENTS AND METHODS IN PHYSICS RESEARCH SECTION A: ACCELERATORS, SPECTROMETERS, DETECTORS AND ASSOCIATED EQUIPMENT **791**, 80 (2015).
- [8] D.A. Brown, M.B. Chadwick, R. Capote et al. , “ENDF/B-VIII.0: The 8th Major Release of the Nuclear Reaction Data Library with CIELO-project Cross Sections, New Standards and Thermal Scattering Data,” NUCL. DATA SHEETS **148**, 1–142 (2018).
- [9] K.J. Kelly, M. Devlin, J.M. O’Donnell et al. , “Measurement of the $^{239}\text{Pu}(n,f)$ prompt fission neutron spectrum from 10 keV to 10 MeV induced by neutrons of energy 1–20 MeV,” PHYSICAL REVIEW C **102**, 034615 (2022).
- [10] P. Marini, J. Taieb, B. Laurent et al. , “Prompt-fission-neutron spectra in the $^{239}\text{Pu}(n,f)$ reaction,” PHYSICAL REVIEW C **101**, 044614 (2022).
- [11] K.J. Kelly, P. Marini, J. Taieb et al. , “Comparison of Results from Recent NNSA and CEA Measurements of the $^{239}\text{Pu}(n, f)$ Prompt Fission Neutron Spectrum,” NUCL. DATA SHEETS **173**, 42–53 (2022).
- [12] J. Bess (editor), “International Handbook of Evaluated Criticality Safety Benchmark Experiments (ICSBEP),” Organization for Economic Co-operation and Development-Nuclear Energy Agency Report NEA/NSC/DOC(95)03 (2019).
- [13] D. Neudecker, V.G. Pronyaev and L. Snyder, “Including $^{238}\text{U}(n,f)/^{235}\text{U}(n,f)$ and $^{239}\text{Pu}(n,f)/^{235}\text{U}(n,f)$ NIFFTE fissionTPC Cross-sections into the Neutron Data Standards Database,” Los Alamos National Laboratory LA-UR-21-24093 (2022).
- [14] D. Neudecker, D.L. Smith, F. Tovesson, et al. , “Applying a template of expected uncertainties to updating $^{239}\text{Pu}(n, f)$ cross-section covariances in the neutron data standards database,” NUCL. DATA SHEETS **163**, 228–248 (2020).
- [15] C. Wong, J.D. Anderson, P. Brown et al. , “Livermore Pulsed Sphere Program: Program Summary through July 1971,” Lawrence Livermore Laboratory Report UCRL-ID-51144 (1972); C. Wong, E.F. Plechaty, R.W. Bauer et al. , “Measurements and Calculations of the Leakage Multiplication from Hollow Beryllium spheres,” Lawrence Livermore Laboratory Report UCRL-ID-91774 (1985); W. Webster and C. Wong, “Measurements of the neutron emission spectra from spheres of N, O, W, ^{235}U , ^{238}U , and ^{239}Pu , pulsed by 14-MeV neutrons,” Lawrence Livermore Laboratory Report UCID-17332 (1976); A.A. Marchetti and G.W. Hedstrom, “New Monte Carlo Simulation of the LLNL Pulsed-Sphere Experiments,” Lawrence Livermore Laboratory Report UCRL-ID-131461 (1998);

- E.R. Plechaty and R.J. Howerton, “Calculation Models for LLL Pulsed Spheres (CSEWG Shielding Benchmark Collection No. SDT 10),” Lawrence Livermore Laboratory Report UCID-16372 (1973).
- [16] D. Neudecker, “ARIADNE—a program estimating covariances in detail for neutron experiments,” EPJ-N **4**, 34 (2018).
- [17] H.-H. Knitter, “Measurement of the Energy Spectrum of Prompt Neutrons from the Fission of Pu 239 by 0.215 MeV Neutrons,” ATOMKERNENERG. **26**, 76–79 (1975), EXFOR-No. 20576.003.
- [18] J. P. Lestone, E. F. Shores, “Uranium and Plutonium Average Prompt-fission Neutron Energy Spectra (PFNS) from the Analysis of NTS NUEX Data”, NUCL. DATA SHEETS **119**, 213–216 (2014).
- [19] J. P. Lestone, E. F. Shores, “Uranium and Plutonium Prompt-fission-neutron Spectra (PFNS) of NTS NUEX Data and the Corresponding Uncertainty Budget”, LANL report **LA-UR-14-24087**, Los Alamos, USA (2014).
- [20] A. Chatillon, G. Belier, T. Granier *et al.* , “Measurement of Prompt Neutron Spectra from the $^{239}\text{Pu}(n, f)$ Fission Reaction for Incident Neutron Energies from 1 to 200 MeV,” PHYS. REV. C **89**, 014611 (2014), EXFOR-No. 14379.
- [21] T. Granier, “Reanalysis of ^{239}Pu Prompt Fission Neutron Spectra,” PHYS. PROCEEDIA **64**, 183–189 (2015).
- [22] M. Sugimoto, A.B. Smith and P.T.Guenther, “Ratio of the Prompt Fission Neutron Spectrum of ^{239}Pu to That of ^{235}U ,” NUCLEAR SCIENCE AND ENGINEERING **97**, 235–238 (1978).
- [23] C.J. Werner *et al.*, “MCNP6.2 Release Notes,” LOS ALAMOS NATIONAL LABORATORY REPORT LA-UR-18-20808 (2018).
- [24] D. Neudecker, O. Cabellos, A.R. Clark, *et al.* , “Which nuclear data can be validated with LLNL pulsed-sphere experiments?,” ANN. NUCL. EN. **159**, 108345 (2021).